THE JOURNAL OF BIOLOGICAL CHEMISTRY
Vol. 256, No. 14, Issue of July 25, pp. 7518-7527, 1981
Printed in U.S.A.

Rotation of Cytochrome Oxidase in Phospholipid Vesicles

INVESTIGATIONS OF INTERACTIONS BETWEEN CYTOCHROME OXIDASES AND BETWEEN CYTOCHROME OXIDASE AND CYTOCHROME bc_1 COMPLEX*

(Received for publication, January 20, 1981)

Suguru Kawato, Erwin Sigel, Ernesto Carafoli, and Richard J. Cherry

From Laboratorium für Biochemie, Eidgenössische Technische Hochschule, ETH-Zentrum, CH-8092 Zürich, Switzerland

Cytochrome oxidase was incorporated into lipid vesicles composed of phosphatidylethanolamine-phosphatidylcholine-cardiolipin. Large proteoliposomes of 1,000-15,000 Å diameter were prepared by calcium-induced fusion of small vesicles. Rotational diffusion of cytochrome oxidase was measured by detecting the decay of the absorption anisotropy, $r(t)$, after photolysis of the heme a_3•CO complex by a vertically polarized laser flash. Because of the large size of the proteoliposomes, there was no contribution of vesicle-tumbling to $r(t)$ over the experimental time range of 5 ms for samples in 60% sucrose. Analysis of $r(t)$ curves was based on a "rotation-about-membrane normal" model. The measurements were used to investigate intermolecular interactions between cytochrome oxidases and between cytochrome oxidase and cytochrome bc_1 complex co-reconstituted in the above lipid vesicles.

In vesicles of a high lipid to protein ratio (≃27), nearly all cytochrome oxidase molecules are rotating with an approximate rotational relaxation time, $\varnothing_1$, on the order of 500 μs. In contrast, about 20% of cytochrome oxidase is immobile in vesicles with a relatively low lipid to protein ratio (≃5), although $\varnothing_1$ of the mobile population remains about 500 μs. The immobilized fraction is presumably due to nonspecific self-aggregation of cytochrome oxidase. The presence of cytochrome bc_1 complex does not change $r(t)$ curves significantly, either in the presence or absence of cytochrome *c*.

Previously, we have observed the co-existence of mobile and immobile populations of cytochrome oxidase in bovine heart and rat heart mitochondria (Kawato, S., Sigel, E., Carafoli, E., and Cherry, R. J. (1980) *J. Biol. Chem.* 255, 5508-5510). The present results suggest that the immobile population of about one-half of cytochrome oxidase could be simply due to nonspecific protein aggregation resulting from the high concentration of enzymes in the inner mitochondrial membrane (lipid to protein ratio, ≤0.5). We also conclude that there is no specific interaction between cytochrome oxidase and cytochrome bc_1 complex in the above large lipid vesicles. A lateral collision-controlled model for electron transfer from cytochrome bc_1 complex to cytochrome oxidase through cytochrome *c* is discussed based on the above results.

Although the kinetics of electron transfer in the respiratory chain in the inner membrane of mitochondria has been extensively studied, the molecular organization and interaction of the respiratory enzymes are not well established (1). Essentially two different types of mechanisms can be considered for electron transfer in the respiratory chain (2); one is that electrons are transferred by collisions between rotationally and laterally diffusing membrane oxidation-reduction components, and the other is that electrons are transferred by tunneling between translationally and rotationally locked components of a multienzyme complex.

Cytochrome oxidase (Complex IV) is the terminal enzyme of the respiratory chain, not only catalyzing the transfer of electrons from cytochrome *c* to molecular oxygen (3, 4) but also pumping protons from the matrix side to the cytoplasmic side across the membrane (5-8). Cytochrome oxidase contains hemes a and a_3 and two copper ions. Heme a_3 is the binding site for CO (9). Cytochrome bc_1 complex (Complex III), which contains two *b* cytochromes, one c_1 cytochrome, iron-sulfur protein, and ubiquinone, catalyzes the transfer of electrons from both Complexes I and II to cytochrome *c* (10-12) and the proton translocation across the membrane (13, 14).

Long range lateral mobility of cytochrome oxidase and other integral proteins has been demonstrated by freeze-fracture electron microscopy (15, 16). Rotational mobility of cytochrome oxidase has recently been demonstrated in the inner membrane of mitochondria by the transient dichroism technique (17) and in reconstituted lipid vesicles by the saturation transfer-electron spin resonance technique (18, 19). We have previously shown that about one-half of cytochrome oxidase is rotating and the other half is relatively immobilized in the mitochondrial membrane (17). The co-existence of mobile and immobile populations of cytochrome oxidase raises an interesting problem, namely whether the immobile population is oligomeric cytochrome oxidase or cytochrome oxidase complexed with other enzymes in the respiratory chain.

Protein rotation is particularly sensitive to protein-protein interactions (20, 21). Here we investigate rotational mobility of cytochrome oxidase and possible intermolecular interactions between cytochrome oxidases and between cytochrome oxidase and cytochrome bc_1 complex in reconstituted lipid vesicles by monitoring cytochrome oxidase rotation. The rotational diffusion measurements of cytochrome oxidase are based on observing flash-induced absorption anisotropy of the heme a_3•CO complex (22). The independent local lateral diffusion of cytochrome oxidase and cytochrome bc_1 complex is discussed on the basis of the rotational mobility.

Since the activity and conformation of cytochrome oxidase are affected by surrounding lipids (23-28), we use phosphatidylethanolamine-phosphatidylcholine-cardiolipin vesicles, corresponding to the major phospholipid components in the mitochondrial inner membrane (29).

EXPERIMENTAL PROCEDURES

Materials

Cytochrome oxidase (EC 1.9.3.1) was prepared from beef heart essentially as described by Yonetani (30) but omitting the last step of

* The costs of publication of this article were defrayed in part by the payment of page charges. This article must therefore be hereby marked "*advertisement*" in accordance with 18 U.S.C. Section 1734 solely to indicate this fact.

the procedure (replacement of cholate by Tween 80). A part of the preparation was further purified on a Sephadex G-200 column with a medium containing 100 mM K phosphate, 2% cholate in order to remove most of the high molecular weight contaminants usually present in cytochrome oxidase preparations. In the following, we call the former and latter preparations "standard oxidase" and "column oxidase," respectively. The heme concentration was about 8–10 nmol of heme a/mg of protein. Heme a was determined using an extinction coefficient of 13.5 mM^{-1} cm^{-1} for reduced minus oxidized heme at the wavelength couple 605–630 nm. The cytochrome oxidase preparations were devoid of other types of cytochromes as judged by spectral data. The enzyme was stored in small portions in buffer containing 100 mM K phosphate (pH 7.4), 2% cholate at a heme a concentration of 200 μM at −80 °C. The activity of isolated cytochrome oxidase was very low but could be activated by the addition of detergent-phospholipid mixtures. Maximal activity was restored when cytochrome oxidase was reconstituted into liposomes.

Cytochrome bc_1 complex was prepared essentially as described by Rieske (31). The enzyme was stored at −80 °C in small aliquots in 50 mM Tris-HCl (pH 8) containing 670 mM sucrose, 1 mM histidine. The heme concentrations were 7.5 nmol of heme b/mg of protein and 4.2 nmol of heme c_1/mg of protein. Hemes b and c_1 were determined using extinction coefficients of 13.2 mM^{-1} cm^{-1} ($\Delta\epsilon_{562-563\ nm}$ (reduced-oxidized)) and 17.5 mM^{-1} cm^{-1} ($\Delta\epsilon_{554-540\ nm}$ (reduced)), respectively.

Horse heart cytochrome *c* (Grade VI) was purchased from Sigma. Phospholipids (egg PC,[1] egg PE, bovine heart CL; all Grade I) were purchased from Lipid Products.

Methods

Preparation of Large Cytochrome Oxidase Vesicles

Reconstitution of Cytochrome Oxidase in Column-formed Vesicles of High L/P = 30—The procedure described by Brunner *et al.* (32) was modified as follows. 40 mg of lipid solution in chloroform-methanol (PE:PC:CL, 1:1:1, by weight) were dried under a N_2 stream and redissolved in diethyl ether. Ether was removed under a N_2 stream and vacuum. The residue was dispersed in 2 ml of a medium which contained 100 mM K-Hepes (pH 7.5), 40 mM KCl, 40 mM K cholate, 0.1 mM K-EDTA. The lipid-detergent mixture was vortexed and sonicated to clarity with a Branson-type sonifier under a N_2 stream with cooling in ice. To 2 ml of the suspension, 60 μl of cytochrome oxidase stock solution were added and vortexed. The resulting solution was applied to a Sephadex G-50m column (1.1 × 43 cm; velocity = 7.3 ml/h, 4 °C). The column was run with the same medium as described above without K cholate. Up to 4 ml of the suspension were applied to the column for a single preparation. The heme-containing fractions were pooled.

Co-reconstitution of Cytochrome Oxidase with Cytochrome bc_1 Complex in Column-formed Vesicles—The same procedure as above was used, except that 50 μl of cytochrome bc_1 complex, containing 11.3 nmol of cytochrome *b*, 6.3 nmol of cytochrome c_1, 1.5 mg of protein, were added together with 60 μl of cytochrome oxidase containing 12 nmol of heme a.

Reconstitution in Column-formed Vesicles at Low L/P = 5—The procedure described above was modified as follows. When cytochrome oxidase was reconstituted alone, 60 μl of cytochrome oxidase were added to 0.3 ml of the sonicated lipid-detergent dispersion (6 mg in lipid). When cytochrome bc_1 complex was reconstituted with cytochrome oxidase, 50 and 60 μl, respectively, of protein stock solution were combined with 0.68 ml of the lipid-detergent dispersion (13.6 mg in lipid). In both cases, the resulting lipid to total protein ratio was 5.

Ca^{2+}-induced Fusion—Ca^{2+}-induced fusion was performed by the method of Miller and Racker (33) with some modifications. Small column-formed vesicles were diluted to 3 to 7 mg of lipids/ml with column medium. After warming to room temperature, 1 M $CaCl_2$ was added to a final concentration of 20 mM. The solution was vortexed and left for 30 min. The Ca^{2+}-induced fusion was stopped by the addition of 0.5 M K-EGTA to a final concentration of 22.5 mM. The pH of the EGTA solution was 9.0 in order to prevent acidification of the resulting solution by protons displaced by calcium ions. The fused vesicles were centrifuged in an Eppendorf bench centrifuge (model 3200, 8000 × *g*) for 5 min. The pellet was diluted to a heme a concentration of about 8 μM. The heme a yield was about 70%. In order to facilitate complete removal of any free Ca^{2+} which might be trapped in interlamellar spaces of multilamellar fused vesicles, the Ca^{2+}-ionophore A_{23187} was added in some experiments.

Protein content was determined from spectroscopic measurements of the heme content. Phospholipid content was determined by phosphorus analysis according to Chen *et al.* (34). It was assumed that the ratio of PE:PC:CL = 1:1:1 was maintained after Ca^{2+}-fusion and pelleting. In this way, we obtained L/P ≃ 27 for high L/P vesicles (starting ratio of L/P = 30) and L/P ≃ 5 for low L/P vesicles (starting ratio of L/P = 5).

Cytochrome oxidase activity was determined in liposomes polarographically by measuring the oxygen consumption in the presence of ascorbate, *N,N,N′,N′*-tetramethyl-*p*-phenylenediamine, and cytochrome *c* after uncoupling by the addition of valinomycin and carbonyl cyanide-*m*-chlorophenyl hydrazone as described in detail elsewhere (8, 35). Cytochrome bc_1 complex activity was determined spectrophotometrically by measuring cytochrome *c* reduction at 550 minus 540 nm after the addition of duroquinol (36). The enzyme activity was determined not only in column-formed PE-PC-CL vesicles but also in asolectin vesicles prepared by the dialysis procedure according to Hinkle *et al.* (37). No significant difference was observed in the enzyme activity between the above two vesicles.

Incorporation of enzymes into lipid vesicles was determined by sucrose density gradient ultracentrifugation. Samples were layered on a discontinuous sucrose density gradient (5, 10, 15, 20, 25, and 30% sucrose (w/w) in K-Hepes medium) in aliquots of about 600 μl (8 μM in heme a)/tube and centrifuged at 150,000 × *g* for 17 h at 2 °C.

For freeze-fracture electron microscopy, samples were jet-frozen from room temperature in liquid propane at a temperature of about −190 °C (38). The cooling rate was on the order of 10^4 °C/s. Freeze-fracture was carried out in Balzer's 300 apparatus. Specimens were replicated with Pt/C and backed with SiO and were examined in a Phillips 200 transmission electron microscope. For negative stain electron micrographs, samples were stained with phosphotungstate.

Gel Filtration Method

For the determination of the size distribution of proteoliposomes before and after the fusion procedure, a Bio-Gel A-150m (Bio-Rad) column (1.6 × 47 cm; *v* = 4.2 ml/h) was used. The column was calibrated with sonicated egg PC liposomes (diameter, 250 Å) and Dow latex particles of uniform size with diameters of 4810 ± 18 Å, 2200 ± 65 Å, and 1090 ± 27 Å. The medium was 100 mM KCl, 10 mM Hepes (pH 7.5), 0.1 mM EDTA. When Dow latex particles were applied to the column, 1% Triton X-100 was included in the medium. 500 μl of five times diluted particles were applied. For determination of the vesicle size of proteoliposomes, 2 ml of proteoliposome suspension with a heme a concentration of 2 μM were applied. The phosphorus in the eluant was analyzed.

Rotational Diffusion Measurements

For rotational diffusion measurements, 60% sucrose was dissolved in proteoliposome suspension; the final heme a concentration was about 2–4 μM. Samples were reduced by 25 mM ascorbate, 50 μM *N,N,N′,N′*-tetramethyl-*p*-phenylenediamine and slowly bubbled for 1 min with CO.

The flash photolysis apparatus used for rotation measurements is described in detail elsewhere (39). Briefly, the sample was excited at 590 nm by a vertically polarized flash of 1–2 μsec in duration from a dye laser (rhodamine 6G in methanol). Absorbance changes due to photolysis of the heme a_3·CO complex were measured at 446–448 nm. The signals were analyzed by calculating the absorption anisotropy, $r(t)$, and the total absorbance change, $A(t)$, given by

$$r(t) = [A_V(t) - A_H(t)]/[A_V(t) + 2A_H(t)] \quad (1)$$

$$A(t) = A_V(t) + 2A_H(t) \quad (2)$$

where $A_V(t)$ and $A_H(t)$, respectively, are the absorbance changes for vertical and horizontal polarization at time *t* after the flash.

In each experiment, 128 signals were averaged using a Datalab DL 102A signal averager. A further improvement in signal-to-noise was achieved by averaging data from a number of experiments. Samples were measured in 60% sucrose solution in order to reduce the rate of vesicle-tumbling and to reduce light scattering. Under the experimental conditions, the effect of light scattering on $r(t)$ and $A(t)$ was negligible.

[1] The abbreviations used are: PC, phosphatidylcholine; ST-ESR, saturation transfer-electron spin resonance; L/P, lipid to protein (w/w) ratio; PE, phosphatidylethanolamine; CL, cardiolipin; RCR, the respiratory control ratio index; Hepes, 4-(2-hydroxyethyl)-1-piperazineethanesulfonic acid; EGTA, ethylene glycol bis(β-aminoethyl ether)-*N,N,N′,N′*-tetraacetic acid.

Analysis of Absorption Anisotropy

Detailed theoretical considerations of rotational diffusion of cytochrome oxidase are presented in miniprint.[2] Here, the theoretical treatment is presented in outline.

Cytochrome oxidase maintains a fixed orientation with respect to the sidedness of the membrane (3, 40), implying that rotation occurs about the normal to the plane of the membrane. Thus, decays in absorption anisotropy, $r(t)$, were analyzed based on a "rotation-about-membrane normal" model (41). A theoretical treatment of this case for heme proteins shows that the expected form of $r(t)$ is given by

$$r(t)/r(0) \equiv r(t)/0.1 = 3 \sin^2 \theta_N \cos^2 \theta_N \exp(-t/\varnothing_\parallel) + \frac{3}{4} \sin^4 \theta_N \exp(-4t/\varnothing_\parallel) + \frac{1}{4}(3 \cos^2 \theta_N - 1)^2 \quad (3)$$

where $\varnothing_\parallel$ is the rotational relaxation time and θ_N is the angle between the membrane normal axis and the normal to the heme plane ($\varnothing_\parallel = 1/D_\parallel$ where $D_\parallel$ is the rotational diffusion coefficient).

Equation 3 expresses the rotation of a single rotating species and assumes 4-fold symmetry of the heme plane. The assumption of 4-fold symmetry is a good approximation in the present experimental condition (*i.e.* excitation at 590 nm and measurement at 446–448 nm) (42). However, the assumption of a single rotating species may not be valid, especially since different populations were found to be present in mitochondrial membranes (17). In the case of multiple populations, the experimental $r(t)$ is the weighted sum of the individual $r(t)$ values with different $\varnothing_\parallel$. Although multiple populations are difficult to resolve, their existence can be inferred by fitting the data by the following general equation

$$r(t) = r_1 \exp(-t/\varnothing_1) + r_2 \exp(-4t/\varnothing_1) + r_3 \quad (4)$$

and comparing r_1, r_2, and r_3 with the theoretical values of Equation 3.

Curve fitting of the data by Equation 4 was accomplished by a Hewlett-Packard HP 9825A desktop computer. It should be noted that in Equations 3 and 4, $r(t)/r(0)$ does not depend on the intensity of photoselecting flash (41) and only $r(0)$ depends on the flash intensity (43). Therefore, $r(t)$ curves obtained at slightly different excitation intensities may be normalized to the same $r(0)$ for a direct comparison in figures.

RESULTS

Activity of Cytochromes in Lipid Vesicles

Both standard and column oxidase have the same specific activity of 40–60 μmol of e^-/min·mg of protein in liposomes of L/P = 30. As a parameter for the quality of the functional reconstitution of cytochromes in column-formed small vesicles, the respiratory control ratio was determined by activity measurements in the presence and absence of valinomycin and carbonyl cyanide-*m*-chlorophenyl hydrazone (44). RCR was 6–8 for standard oxidase with L/P = 30 and larger than 6 for cytochrome bc_1 complex with L/P = 15. These results suggest that nearly all (>80%) cytochrome oxidase and cytochrome bc_1 complex are functionally incorporated in liposomes by the cholate column method. However, a relatively low RCR (≤4) was observed for column oxidase with L/P = 30, although there was no decrease in the oxygen consumption activity for column oxidase compared with standard oxidase. Because of the multilamellar structure of Ca^{2+}-fused pellet vesicles, we could not measure the activity and RCR of cytochrome oxidase and cytochrome bc_1 complex in these vesicles.

The effect of 60% sucrose on the activity and RCR of cytochrome oxidase in column-formed vesicles was checked. After a 1-h incubation in 60% sucrose, the sample was diluted to 10% sucrose by the addition of buffer solution, and the activity and RCR were measured. No significant decrease in either the oxygen consumption activity or RCR was observed. Since all flash photolysis experiments were performed within 1 h after suspending vesicles in 60% sucrose, no degradation of enzymes due to sucrose can be expected during transient dichroism measurements.

Vesicle Size Distribution

Since PE, PC, and CL comprise 98% of total phospholipids with a weight ratio of PE:PC:CL ≃ 40:35:50 in the inner membrane of bovine heart mitochondria (29), we chose PE:PC:CL = 1:1:1 vesicles for the present experiments. PE and negatively charged lipids are important for an effective Ca^{2+}-induced fusion procedure (33).

Fig. 1 illustrates the elution pattern of cholate column proteoliposomes before and after the fusion procedure. The main peak of nonfused vesicles is around 250–350 Å, and less than 13% of phospholipids is contained in vesicles with diameters larger than 950 Å. After fusion and pelleting, more than 92% of lipids elutes in the fraction with a particle diameter larger than 950 Å. An accurate size distribution of Ca^{2+}-fused pellet vesicles cannot be obtained from these data, since most phospholipids elute very close to the void volume and are not resolved on the column.

As judged by freeze-fracture and negative stain electron micrographs, Ca^{2+}-fused pellet vesicles were distributed between 1,000–15,000 Å in diameter. Moreover, it was observed that pellet vesicles have a multilamellar structure.

Incorporation of Proteins into Lipid Vesicles

Incorporation of enzymes into lipid vesicles can be demonstrated by gradient centrifugation in sucrose. A variety of proteoliposomes was centrifuged into a step sucrose gradient.

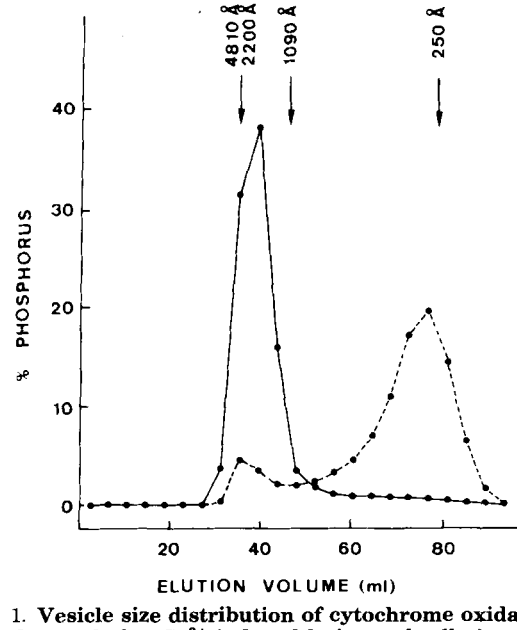

FIG. 1. **Vesicle size distribution of cytochrome oxidase vesicles before and after Ca^{2+}-induced fusion and pelleting.** Elution profiles on a Bio-Gel A-150m column of small proteoliposomes prepared by cholate column procedures (*dashed line*) and large proteoliposomes prepared by Ca^{2+}-induced fusion and pelleting from column-formed small vesicles (*solid line*). Detailed procedures for vesicle preparations are described under "Experimental Procedures." Calibration of the Bio-Gel column was performed by sonicated egg PC liposomes (250 Å) and Dow latex particles (1090 Å, 2200 Å, 4810 Å).

[2] Portions of this paper (including "Theoretical Treatment of Rotation of Cytochrome Oxidase in Membranes" and Fig. 4) are presented in miniprint at the end of this paper. Miniprint is easily read with the aid of a standard magnifying glass. Full size photocopies are available from the Journal of Biological Chemistry, 9650 Rockville Pike, Bethesda, MD 20014. Request Document No. 81M-125, cite author(s), and include a check or money order for $2.00 per set of photocopies. Full size photocopies are also included in the microfilm edition of the Journal that is available from Waverly Press.

Ca^{2+}-fused pellet vesicles showed a single band regardless of the amount of lipid added to enzymes, while column-formed small vesicles had a variety of subpopulations. The co-reconstitution of cytochrome oxidase and cytochrome bc_1 complex in Ca^{2+}-fused pellet vesicles was demonstrated by the change in the density of cytochrome oxidase vesicles in the presence of cytochrome bc_1 complex (see Fig. 2). Furthermore, the band which was isolated from the Fig. 2*b* sample showed the spectral characteristics of both cytochrome oxidase and cytochrome bc_1 complex.

Ultrastructural Analysis

Distribution of cytochrome oxidase molecules in Ca^{2+}-fused pellet vesicles was investigated by freeze-fracture electron microscopy. Fig. 3 shows typical examples of proteoliposomes containing cytochrome oxidase jet-frozen from room temperature (cooling rate ~ 10^4 °C/s). On the photograph, intramembranous particles are visible, whereas these are not detected in control liposomes which were prepared without addition of proteins. Therefore, these particles represent cytochrome oxidase; however, it is not known whether or not the smallest particles in the photograph represent monomers, dimers, or oligomers of cytochrome oxidase.

In Fig. 3, although there is a wide variety of particle sizes, the majority of membrane particles is about 100 Å in diameter, and there are almost no particles larger than 300 Å in L/P ≃ 27 vesicles containing standard oxidase. In contrast, relatively large microaggregates larger than 500 Å in length can be easily observed in both L/P ≃ 27 column oxidase vesicles and L/P ≃ 5 standard oxidase vesicles. Thus, the formation of microaggregates appears to depend on both the lipid to protein ratio and the difference in purification procedure of cytochrome oxidase.

Characterization of Rotational Diffusion of Cytochrome Oxidase

All of the following $r(t)$ measurements were performed in Ca^{2+}-fused pellet vesicles unless otherwise stated, since there is no contribution of vesicle-tumbling to $r(t)$ curves in these large vesicles (see the following section). In these vesicles, all $r(t)$ curves decayed within 2 ms to a time-independent value $r(\infty)$ (see Fig. 7).

Slow rotational diffusion of membrane proteins may conceivably consist of two different modes; one is wobbling of part of the protein molecule or the whole protein molecule, and the other is rotation of the protein molecule about the membrane normal. In the present case of cytochrome oxidase, the theoretically predicted $r(\infty)/r(0)$ is about 0.25 from Equation 3 with the rotation-about-membrane normal model, since the heme a_3 plane is close to perpendicular to the plane of the membrane ($\theta_N \simeq 90°$ in Equation 3) (45, 46). Possible segmental wobbling and/or a rocking motion of cytochrome oxidase molecule about axes in the plane of the membrane should further decrease $r(\infty)/r(0)$ to below 0.25. The measured lowest value, $r(\infty)/r(0) = 0.28 \pm 0.02$, in high L/P vesicles therefore

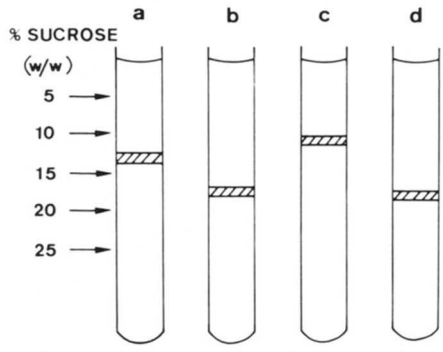

FIG. 2. **Analysis of incorporation of enzymes into PE-PC-CL vesicles by centrifugation in sucrose density gradient.** Large proteoliposomes were prepared by Ca^{2+}-induced fusion and pelleting as described under "Experimental Procedures." Proteoliposomes were centrifuged into discontinuous sucrose gradients. Enzymes in vesicles were: *a*, standard oxidase (L/P ≃ 10); *b*, standard oxidase + cytochrome bc_1 complex (heme a:heme b = 1:1, L/P ≃ 5); *c*, standard oxidase (L/P ≃ 27); *d*, standard oxidase (L/P ≃ 5). *a* is the control experiment of *b*.

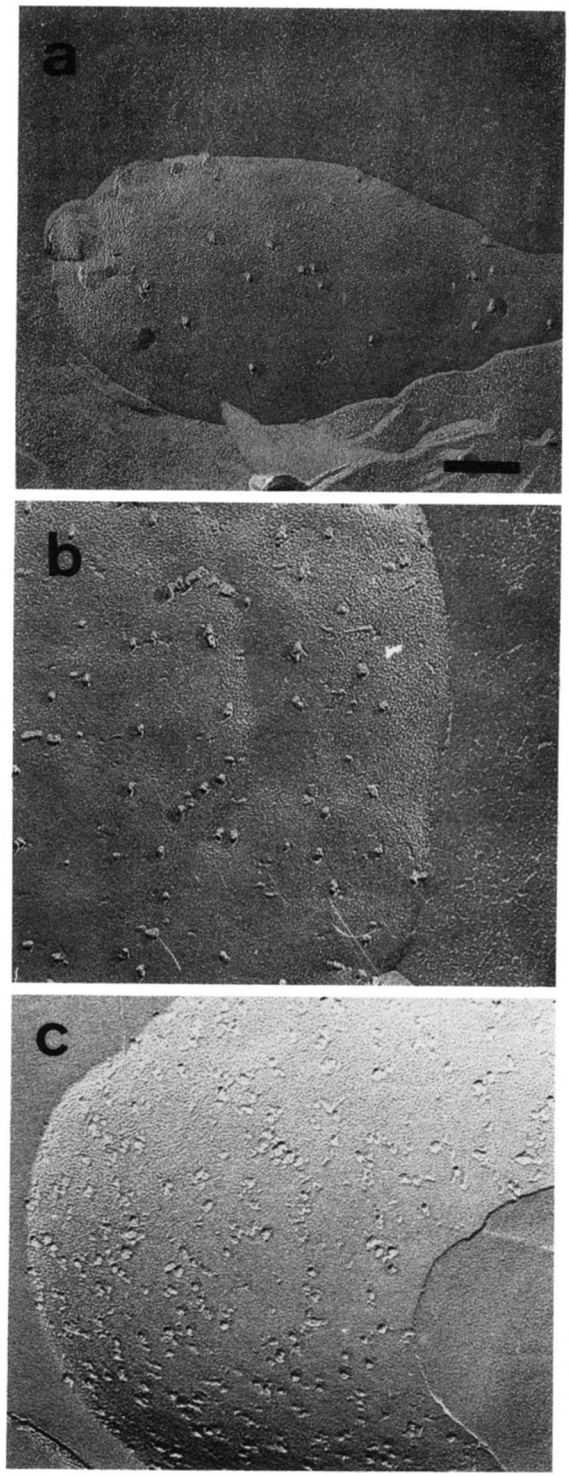

FIG. 3. **Freeze-fracture electron micrographs of cytochrome oxidase vesicles prepared by Ca^{2+}-induced fusion and pelleting procedures.** *a*, standard oxidase vesicles (L/P ≃ 27); *b*, column oxidase vesicles (L/P ≃ 27); *c*, standard oxidase vesicles (L/P ≃ 5). The *bar* indicates 1000 Å.

eliminates the possibility of the above segmental flexibility and rocking motion of cytochrome oxidase (see Table I).

No effect of the addition of Ca^{2+} ionophore with excess amount of EGTA was observed on $r(t)$ curves, implying that all Ca^{2+}, which possibly remained in interlamellar spaces in these multilamellar vesicles, was already chelated by EGTA during vesicle preparation (see "Experimental Procedures").

Effect of Lipid to Protein Ratio—Rotational diffusion of standard cytochrome oxidase was measured with varying L/P. Fig. 5 shows typical $r(t)$ curves. Data were analyzed by Equation 4 and decay parameters are summarized in Table I. The time-independent normalized residual anisotropy $r_3/r(0)$ is closely related to the population of immobile cytochrome oxidase. If we assume that the heme a_3 plane is perpendicular to the plane of the membrane ($\theta_N = 90°$ in Equation 3), an immobile fraction (f_{im}) can be calculated as follows

$$r_3/r(0) = f_{im} \cdot 1 + (1 - f_{im}) \cdot 0.25 \quad (5)$$

TABLE I

Decay parameters of time-dependent absorption anisotropy of cytochrome oxidase in a variety of proteoliposomes analyzed by Equation 4

All measurements except mitochondria were performed with Ca^{2+}-fused pellet vesicles in 60% sucrose solution.

Enzymes in vesicles	L/P	$\varnothing_1$	$r_3/r(0)$	Immobile oxidase[a]	r_1/r_2	Temperature
		μs		%		°C
Standard oxidase	27	517 (46)[b]	0.28 (0.02)	4 (3)	1.0 (0.2)	22
Standard oxidase + bc_1[c]	15	509 (51)	0.30 (0.01)	7 (2)	1.0 (0.2)	22
Standard oxidase	5	460 (24)	0.38 (0.01)	17 (2)	1.6 (0.1)	20
Standard oxidase + bc_1	5	506 (34)	0.41 (0.01)	21 (2)	1.3 (0.3)	20
Column oxidase	27	521 (60)	0.47 (0.01)	29 (2)	1.4 (0.3)	22
Standard oxidase + bc_1	5	582 (31)	0.43 (0.01)	24 (2)	2.5 (0.4)	5
Bovine heart mitochondria[d]	0.39	350 (20)	0.54 (0.05)	39 (7)	2.5 (1.4)	37

[a] The percentage of immobile population of cytochrome oxidase was calculated based on Equation 5.

[b] Numbers in parentheses, standard deviation.

[c] bc_1, cytochrome bc_1 complex.

[d] Bovine heart mitochondria were measured in 50% sucrose solution. Decay parameters of mitochondria are taken from Kawato *et al.* (17).

Nearly all cytochrome oxidases are rotating in L/P ≃ 27 vesicles with a rotational relaxation time $\varnothing_1 \simeq 500$ μs. A decrease in L/P from 27 to 5 increases the population of immobile cytochrome oxidase up to 17%, while $\varnothing_1$ essentially remains unchanged within experimental error. Equation 3 shows that r_1/r_2 is equal to 4 $\cot^2 \theta_N$ when there is a single rotating species, so that r_1/r_2 should be close to zero for cytochrome oxidase ($\theta_N \simeq 90°$). Actually r_1/r_2 is, however, larger than 1.0 in all cases examined. This strongly suggests that there are heterogeneous rotating species, which is consistent with the different oligomeric membrane particles in freeze-fracture pictures (see Fig. 3). In this case, r_1/r_2 should be regarded as a parameter which represents a rough ratio of a slowly rotating oxidase to a rapidly rotating oxidase. Taking into account the freeze-fracture investigations, monomeric and/or dimeric membrane particles may correspond to the rapidly rotating species and larger oligomers may correspond to the slowly rotating species. However, if oligomers are longer than a rod-shaped heptamer, these might be detected as an immobile population.

Effect of Cytochrome bc_1 Complex—Protein-protein interactions were investigated in standard oxidase + bc_1 co-reconstituted vesicles. In both lipid-rich vesicles (L/P ≃ 27) and lipid-poor vesicles (L/P ≃ 5), the rotational relaxation time, r_1/r_2, and the population of the immobile cytochrome oxidase all essentially remained unchanged. However, the immobile population of cytochrome oxidase could be systematically slightly larger in the presence of cytochrome bc_1 complex (see Table I). In L/P ≃ 15 vesicles, this might be due to the decrease in L/P from 27 to 15, because cytochrome bc_1 is added at a constant lipid to oxidase ratio of 30. In L/P ≃ 5 vesicles, the lipid to total protein ratio was kept at 5 in both the presence and absence of cytochrome bc_1 complex, so that the lipid to oxidase ratio in oxidase + bc_1 vesicles was one-half of that in oxidase vesicles. Nevertheless, the immobile fraction of cytochrome oxidase was almost the same in the above two different vesicles, implying that the immobile fraction of cytochrome oxidase depends not on the lipid to oxidase ratio but on the lipid to total protein ratio.

There was little effect (≲5% change) on $\varnothing_1$, r_1/r_2, and the immobile fraction of cytochrome oxidase by the addition of cytochrome *c* to standard oxidase + bc_1 (L/P ≃ 5) samples. Cytochrome *c* (50 μM) was added to column-formed small vesicles prior to Ca^{2+}-induced fusion.

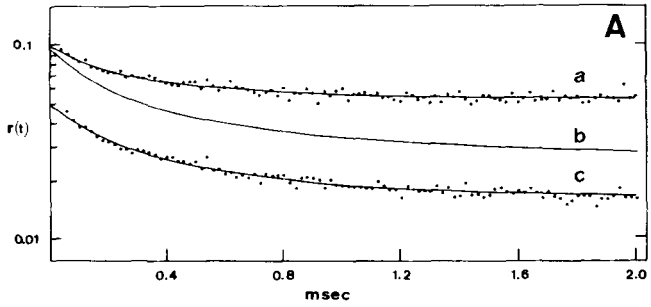

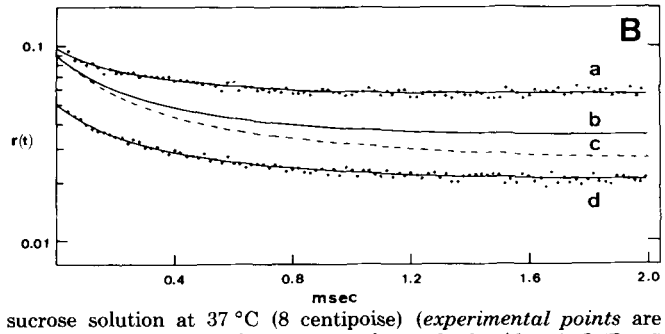

FIG. 5. **Time-dependent absorption anisotropy of the cytochrome oxidase•CO complex in PE-PC-CL vesicles.** Samples (2–4 μM in heme a) were photolyzed by a vertically polarized laser flash at 590 nm, and $r(t)$ was recorded at 446 nm as described under "Experimental Procedures." All measurements were performed with Ca^{2+}-fused pellet large vesicles in 60% sucrose solution at 20–22 °C (55–58 centipoise). *A*, L/P ≃ 27 vesicles. *Curve a*, column oxidase vesicles; *curve b*, standard oxidase vesicles; *curve c*, standard oxidase + cytochrome bc_1 complex vesicles. *Solid lines* were obtained by fitting the data to Equation 4. *Data points* of *curve b* are omitted for clarity. The initial anisotropy of *curve c* is adjusted to $r(0) = 0.05$ for illustrative purposes; otherwise, *curve c* is almost completely superimposed on *curve b*. *B*, *curve a*, bovine heart mitochondria in 50% sucrose solution at 37 °C (8 centipoise) (*experimental points* are taken from Kawato *et al.* (17)); *curve b*, standard oxidase in L/P ≃ 5 vesicles; *curve c*, standard oxidase in L/P ≃ 27 vesicles; *curve d*, standard oxidase + cytochrome bc_1 complex in L/P ≃ 5 vesicles. *Solid lines* were obtained by fitting the data to Equation 4. Almost the same $r(t)$ curves for bovine heart mitochondria were obtained in both 50% sucrose solution at 37 °C and 60% sucrose solution at 20 °C. *Curve c* is taken from *A* and the $r(0)$ is adjusted to the same value as that of *curve b*. The initial anisotropy of *curve d* is adjusted to $r(0) = 0.05$ for illustrative purposes; otherwise, *curve d* is almost completely superimposed on *curve b*. *Experimental points* of *curves b* and *c* are omitted for clarity.

Column-purified Cytochrome Oxidase—Rotational diffusion characteristics of column oxidase was significantly different from standard oxidase in L/P ≃ 27 vesicles. Although $\varnothing_1$ and r_1/r_2 are quite similar to each other, 30% of column oxidase is immobilized in such lipid-rich vesicles. The above immobile population is clearly larger than that of standard oxidase in L/P ≃ 5 vesicles. These immobile oligomers are presumably a consequence of irreversible aggregation of the enzyme during further purification by a Sephadex column. This is interesting because we observed relatively low RCR (≤4) for column oxidase in small column-formed vesicles, and this may also be a consequence of the existence of irreversible aggregates.

Effect of Temperature, Glutaraldehyde Fixation, and Ca^{2+}—Since the present PE-PC-CL vesicles were in the liquid-crystalline state above 0 °C, as demonstrated by fluorescence polarization measurements with diphenylhexatriene,[3] the effect of lowering the temperature from room temperature to 5 °C was not remarkable. For example, in standard oxidase + bc_1 vesicles with L/P ≃ 5, an increase in the immobile fraction of cytochrome oxidase due to decreasing the temperature from 20 to 5 °C is negligible; however, the parallel increase in $\varnothing_1$ and r_1/r_2 suggests the formation of small microaggregates induced by a decrease in temperature (see Table I).

Because better signal-to-noise is obtained at lower temperatures, the effect of glutaraldehyde and Ca^{2+} was examined at 5 °C. Glutaraldehyde fixation (4%) on standard oxidase vesicles (L/P ≃ 27) produced up to 50% of immobile cytochrome oxidase and changed r_1/r_2 from 1.0 to 8 without a significant change in $\varnothing_1$. On the other hand, the addition of 17 mM Ca^{2+} to standard oxidase + bc_1 vesicles (L/P ≃ 15) increased the immobile population of cytochrome oxidase up to 55% without changing r_1/r_2 and $\varnothing_1$ significantly.

Rotation in Isotropic Solution—A large difference in decay characteristics of $r(t)$ was observed between standard oxidase and column oxidase in detergent solution containing 2% cholate in the presence of 60% sucrose (see Fig. 6). In such isotropic solution, $r(t)$ should reach zero, if all enzymes are rotating. From Fig. 6, we conclude that all standard oxidase molecules are thus rotating with a rotational correlation time, $\varnothing$, faster than 200 μs. In contrast, a time-independent residual anisotropy was observed in $r(t)$ for column oxidase, implying that a fraction of column oxidase is immobile due to large aggregates (>500 Å in diameter). Moreover, even when we used a very weak flash excitation in order to prevent the decrease in $r(0)$ due to an intense flash excitation (41), the measured $r(0)$ values for both standard and column cytochrome oxidase were relatively low, about 0.07. This suggests that there are rapidly rotating populations of cytochrome oxidase ($\varnothing \lesssim 10$ μs), which were not detected with the present time resolution.

Vesicle-tumbling

Rotational diffusion characteristics of cytochrome oxidase were examined in small column-formed vesicles, Ca^{2+}-fused vesicles without pelleting, and large Ca^{2+}-fused pellet vesicles (see Fig. 7). The decay characteristics of $r(t)$ curves were different among these three vesicles. Although in these three samples $r(t)$ decayed within 3 ms to a time-independent value, the time-independent normalized residual anisotropy $r(\infty)/r(0)$ depends on the sample. As discussed already, according to the rotation-about-membrane normal model (Equation 3) the smallest value of $r(\infty)/r(0)$ for cytochrome oxidase should be about 0.25. However, both column-formed vesicles and Ca^{2+}-fused vesicles had lower $r(\infty)/r(0)$, ≃0.12 and ≃0.17, respectively, than the 0.25 value. This is probably due to the contribution of vesicle-tumbling to the decay of $r(t)$, since the rotational correlation time of 300 Å vesicles can be calculated as about 200 μs in 60% sucrose at 22 °C (55 centipoise) and these vesicles are the major component in column-formed vesicles and a fraction in Ca^{2+}-fused vesicles without pelleting as judged by Bio-Gel A-150m gel filtration, negative stain electron microscopy, and freeze-fracture electron microscopy.

The rotational correlation time of Ca^{2+}-fused pellet vesicles can be calculated as slower than 7 ms in 60% sucrose. In fact, 60% sucrose introduced aggregation of vesicles as judged by negative stain electron microscopy, so that the actual tumbling rate is probably even slower. Actually, a double exponential best fit for $r(t)$ of Ca^{2+}-fused pellet vesicles showed that the slow decaying component had a rotational correlation time larger than 100 ms, so that the vesicle-tumbling of pellet vesicles is slower than 100 ms. Thus, we have used Ca^{2+}-fused pellet large vesicles for investigations of rotation of cytochrome oxidase, where we can eliminate completely the contribution of vesicle-tumbling.

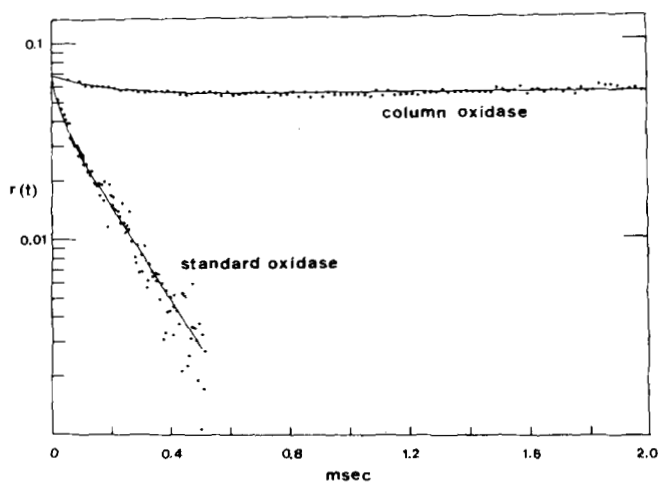

FIG. 6. **Time-dependent absorption anisotropy of cytochrome oxidase in detergent solution.** Measurements were performed in phosphate buffer containing 2% cholate, 60% sucrose at 20 °C (58 centipoise). *Upper curve*, column oxidase; *solid line*, the best fit curve of $r(t) = 0.014 \exp(-t/201\ \mu s) + 0.053$. *Lower curve*, standard oxidase; *solid line*, the best fit curve of $r(t) = 0.023 \exp(-t/30\ \mu s) + 0.045 \exp(-t/180\ \mu s)$.

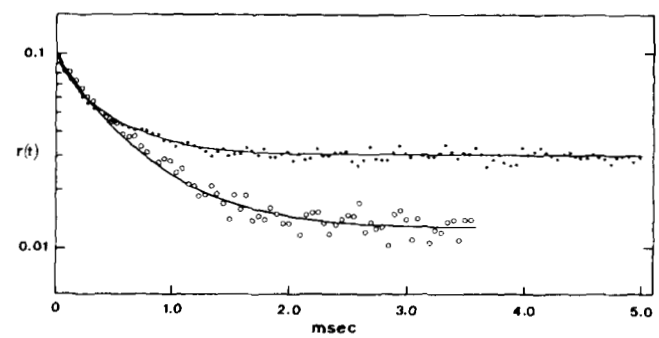

FIG. 7. **Time-dependent absorption anisotropy of cytochrome oxidase in PE-PC-CL vesicles before and after Ca^{2+}-induced fusion and pelleting.** Measurements were performed in 60% sucrose solution at 22 °C (55 centipoise). *Upper curve*, standard oxidase in Ca^{2+}-fused pellet large vesicles; *lower curve*, standard oxidase in column-formed small vesicles. *Solid lines* were obtained by fitting the data to Equation 4. The initial anisotropy of these two *curves* is adjusted to $r(0) = 0.1$ in order to allow a direct comparison. This adjustment is allowed because these two $r(t)$ curves were measured at different excitation flash intensities, which resulted in a shift of the whole $r(t)$ curve (41).

[3] S. Kawato, unpublished results.

Rebinding Kinetics of CO to Reduced Heme a_3

In the present experiments, the sample was bubbled for 1 min by CO and then equilibrated for 30 min in a quartz cuvette sealed by a rubber cap. Thus, the sample was saturated with CO, and all cytochrome oxidase should exist as the heme a_3·CO complex. The rebinding kinetics of CO to reduced heme a_3 after photolysis was monoexponential. The time constant, τ, of this reaction of reduced heme a_3 with CO was almost the same, irrespective of whether cytochrome oxidase is in PE-PC-CL vesicles (with and without cytochrome bc_1 complex and/or cytochrome *c*), detergent solution, mitochondria, or submitochondrial particles. The time constant of reaction, τ, depends only on the solvent viscosity with $\tau = 10 \pm 1$ ms in 60% sucrose at 20–22 °C (55–58 centipoise) and $\tau = 6 \pm 1$ ms in 50% sucrose at 37 °C (8 centipoise).

The above monoexponential reaction kinetics of reduced heme a_3 with CO was different from the double exponential reaction kinetics of reduced hemoglobin and cytochrome P-450 with CO in 60% sucrose.[3] The time constants are $\tau_1 \sim 0.4$ ms, $\tau_2 \sim 1$ msec for human hemoglobin and $\tau_1 \sim 0.2$ ms, $\tau_2 \sim 2$ ms for cytochrome P-450 in rat liver microsomes in 60% sucrose at 20 °C. The reaction of heme a_3 with CO is slowest of the above three hemes, implying that the heme a_3 pocket in cytochrome oxidase is relatively inaccessible to ligands.

DISCUSSION

Rotation and Intermolecular Interactions of Cytochrome Oxidase in Lipid Vesicles and Mitochondrial Inner Membranes—Two different types of cytochrome oxidase preparations were used in the present investigations; one is standard oxidase prepared according to the method of Yonetani (30), and the other is column oxidase which was obtained by the further purification of standard oxidase with a Sephadex column (see "Materials"). In detergent solution in the presence of 60% sucrose, more than one-half of column oxidase exists as large aggregates which are immobile in the present time range. Even after the incorporation into vesicles of relatively high L/P ≃ 27, 30% of column oxidase remains immobile. The existence of large microaggregates of column oxidase in PE-PC-CL vesicles as judged by freeze-fracture pictures supports the above results. Similar phenomena have been observed by Swanson *et al.* (19), who have found that rotationally immobile unchromatographed Triton X-100 preparations of cytochrome oxidase in detergent solution are also immobile in egg lecithin and/or mitochondrial lipid vesicles (rotational time constant ≳1 ms). Thus, in order to prepare rotationally mobile cytochrome oxidase in reconstituted lipid vesicles, it is important to use a detergent solution in which large microaggregates of cytochrome oxidase are essentially absent.

Standard oxidase is suitable for investigations of intermolecular interactions, because nearly all standard oxidase (>95%) is rotating in L/P ≃ 27 vesicles as well as in detergent solution. Any slowing down in rotation and/or immobilization of standard oxidase due to changes in membrane composition can therefore be interpreted as an effect of protein-protein interactions. We have found that the fraction of mobile standard oxidase depends on the lipid to total protein ratio. A decrease in L/P from 27 to 5 increases the immobile population from ~5 to ~20%. This increase in the immobile population coincides with an increase in the number of large microaggregates of standard oxidase in L/P ≃ 5 vesicles as judged by freeze-fracture electron micrographs.

The preceding results with different L/P ratios demonstrate that an increase in the concentration of enzymes in the membrane can induce an immobilization of cytochrome oxidase which is presumably due to nonspecific protein aggregation. Since the inner membrane of bovine heart mitochondria has very low L/P ≃ 0.39 (29), it would be expected that the fraction of immobile cytochrome oxidase would be considerably greater than the 20% observed in the present experiments with L/P ≃ 5 vesicles. Thus, it may not be necessary to assume the existence of any special complex of cytochrome oxidase with other enzymes in the respiratory chain, in order to explain the immobile population of about 50% of cytochrome oxidase previously detected in the inner membrane of mitochondria (17).

Effect of Cytochrome bc_1 Complex on Rotation of Cytochrome Oxidase—The rotational relaxation time is very sensitive to the size of a protein. In the case of rotation about the normal to the plane of the membrane, treating the protein as a cylinder, the relaxation time $\varnothing_\parallel$ is proportional to the square of the protein radius (47)

$$\varnothing_\parallel = 4\pi a^2 h\eta/kT \tag{6}$$

where a is the radius of the cylinder, h is the length immersed in the membrane, η is the membrane viscosity, k is the Boltzmann constant, and T is the absolute temperature. Thus, if cytochrome oxidase forms a stable complex with cytochrome bc_1 complex, a significant change in the $r(t)$ curve should be observable in the presence of cytochrome bc_1 complex.

Cytochrome bc_1 complex is a large integral protein of $M_r = \sim 2.7 \times 10^5$ which contains two b hemes and one c_1 heme (10). Very recently, the three-dimensional structure of cytochrome bc_1 complex from *Neurospora* mitochondria has been investigated (48, 49). The monomeric cytochrome bc_1 complex is a cylindrical protein of height ~140 Å and diameter ~40 Å in the membrane-embedded region. On the other hand, a deoxycholate-treated cytochrome oxidase molecule, which contains heme a and a_3, has been shown to resemble a lopsided "Y" of height ~110 Å and diameter ~70 Å in the membrane-embedded region (40, 50). Thus, a one to one hypothetical complex of cytochrome oxidase (heme aa_3) molecule with cytochrome bc_1 complex (heme 2b + c_1) molecule could have around 1.5 times the diameter of cytochrome oxidase resulting in a 2–3-fold increase in the rotational relaxation time.

In the present experiments, we have added equimolar cytochrome bc_1 (heme 2b + c_1) molecule to cytochrome oxidase (heme aa_3) molecule in both L/P ≃ 15 and L/P ≃ 5 vesicles. If these cytochromes form a one to one stable supercomplex, the expected increase in relaxation time should be detectable as either an increase in $\varnothing_1$ or an marked increase in the ratio r_1/r_2 in Equation 4. The present data show, however, almost no increase in both $\varnothing_1$ and r_1/r_2, suggesting that cytochrome oxidase does not form a specific complex with cytochrome bc_1 complex. Moreover, these parameters remain essentially unchanged in the presence of cytochrome *c*, indicating that cytochrome *c* does not induce stable complex formation between cytochrome oxidase and cytochrome bc_1 complex.

Rotational Diffusion of Cytochrome Oxidase Investigated by Other Physical Techniques—Recently, rotational mobility of cytochrome oxidase has been demonstrated by ST-ESR in asolectin vesicles, mitochondrial lipid vesicles, and egg lecithin vesicles (18, 19). A rotational time constant of about 40 μs at 4 °C was obtained in the above vesicles by comparison with calibration spectra for isotropic rotation. It should be noted that, in general, an isotropic rotation approximation should give a larger value for a rotational time constant than does an anisotropic rotation analysis. However, ST-ESR results showed considerably smaller time constants than values of $\varnothing_1$ (350–600 μs) obtained in our experiments (17). Since we obtained similar $\varnothing_1$ values over a wide range of solution viscosity (8–180 centipoise), it is unlikely that the large difference in the rotational time constant between our results and

ST-ESR results is due to the presence of 60% sucrose in our present experiments.

Kawato *et al.* (27, 28) have observed a biphasic decay in the time-dependent fluorescence anisotropy for cytochrome oxidase labeled by a fluorescent SH reagent in Emasol cholate phosphate solution. The very rapid decay on the order of 1 ns was due to independent wobbling of a fluorescent probe, while the rotational correlation time of the whole protein was around 150 ns. This value is reasonable for the monomeric heme aa_3 molecule ($M_r = \sim 2 \times 10^5$ in Emasol cholate phosphate solution) (51). Rotational correlation times of ~100 ns (19) and ~25 ns (18) have been observed by ST-ESR for detergent-solubilized cytochrome oxidase. We have observed isotropic rotation of standard oxidase in detergent solution containing 60% sucrose (58 centipoise at 20 °C) (see Fig. 6). The measured rotational correlation times $\varnothing_1 = 30$ μs and $\varnothing_2 = 180$ μs correspond to ~500 ns and ~3000 ns in 1 centipoise solution, respectively, implying that standard oxidase forms a variety of aggregates in detergent solution.

Local Lateral Diffusion of Cytochrome Oxidase—Long range lateral diffusion of membrane proteins may be measured by fluorescence photobleaching recovery (52–54). So far, no methods exist for direct measurement of the local lateral diffusion.

The mitochondrial inner membranes are densely packed with integral proteins with around one-third of the total membrane area occupied by integral membrane proteins (29, 55–57). This suggests that the electron transfer between enzymes in the respiratory chain may not need long range lateral diffusion but is controlled by local lateral collisions.

The present rotational relaxation time, $\varnothing_\parallel$, can be related to the local (free) lateral diffusion coefficient (D_L^{loc}) by the following expression (47)

$$D_L^{loc} \simeq (\ln \eta/\eta' - \gamma) \cdot a^2/\varnothing_\parallel \quad (7)$$

where η is the membrane viscosity, η' is the viscosity of the aqueous phase, and γ is the Euler's constant (0.5772). As discussed in the previous section, the measured $\varnothing_1$ is not an exact $\varnothing_\parallel$ but probably represents an average value over different rotating species of cytochrome oxidase. If we take $a \sim 70$ Å (radius intermediate between monomeric and dimeric particles), $\varnothing_\parallel \simeq 500$ μs, $\eta \sim 500$ centipoise, and $\eta' \sim 60$ centipoise, we obtain $D_L^{loc} \simeq 2 \times 10^{-9}$ cm²/s for mobile cytochrome oxidase in lipid vesicles. A similar D_L^{loc} may be obtained in the intact mitochondrial membrane with $\varnothing_\parallel \simeq 350$ μs (17). Since the lateral diffusion coefficient is very insensitive to the particle radius (47), even rotationally immobile microaggregates (~1000 Å in length) would be expected to have similar magnitude of D_L^{loc}. This value for D_L^{loc} is at least an order of magnitude larger than the long range lateral diffusion coefficient for many integral membrane proteins examined ($D_L \lesssim 10^{-10}$ cm²/s) (58). These lower diffusion coefficients have principally been obtained with whole cells and may indicate restrictions to long range diffusion by cytoskeletal structures (58).

Cytochrome bc_1 complex is a transmembrane protein, implying that rotation only occurs about the membrane normal. Moreover, as was mentioned in the previous section, the shape of the membrane-immersed region is not very different between cytochrome oxidase and cytochrome bc_1 complex (49, 50), so that D_L^{loc} for cytochrome bc_1 complex is presumably also on the order of 10^{-9} cm²/s.

On the other hand, a small peripheral protein cytochrome *c* ($M_r = 12{,}398$) could diffuse comparatively rapidly on the surface of the membrane. Membrane-bound amphipathic apolipoprotein ApoC-III ($M_r = \sim 9000$) has been shown to rapidly diffuse on the surface of egg lecithin bilayers with $D_L \simeq 3 \times 10^{-8}$ cm²/s at 20 °C, which is similar to D_L of lipid probes (59). Taking into account this result, D_L^{loc} of cytochrome *c* on the membrane surface might be on the order of 10^{-8} cm²/s.

Assuming the molecular weight of heme aa_3 molecule as 2×10^5, the average inner membrane area/heme aa_3 of about 40,000 Å² can be swept within ~5 ms by cytochrome oxidase and cytochrome bc_1 complex and within ~0.5 ms by cytochrome *c*. Therefore, at least several collisions between these molecules could occur within the time required by the known rates of electron transfer, for example, ~25 ms/e^-/heme aa_3 (duroquinol → cytochrome bc_1 complex → cytochrome c → cytochrome oxidase → molecular oxygen) (60).

Electron Transfer from Cytochrome bc_1 Complex to Cytochrome Oxidase in the Inner Membrane of Mitochondria—Although we find a large difference in rotational mobility between standard oxidase and column oxidase, no difference is observed in the oxygen consumption activity. Similar results of Swanson *et al.* (19) have shown that chromatographed dissociated cytochrome oxidase treated by Triton X-100 is rotating with a time constant of about 40 μs, while unchromatographed cytochrome oxidase is immobilized within their ST-ESR time range (rotational time constant ≳ 1 ms). Moreover, they have observed no difference in the oxygen consumption activity between the above mobile and immobile cytochrome oxidases. Schneider *et al.* (61) have developed a technique for enriching lipids into the inner membrane of rat liver mitochondria by pH-induced fusion with pure liposomes. They have shown that an increase in L/P and in average distance between integral membrane proteins does not decrease the oxygen consumption activity of cytochrome oxidase but even slightly increases it. Thus, as far as the electron transfer from cytochrome *c* to molecular oxygen through cytochrome oxidase is concerned, we can conclude that the mobility of cytochrome oxidase is not rate-limiting for this electron transfer.

The electron transfer activity from duroquinol to molecular oxygen through cytochrome *b*, c_1, *c*, and aa_3 was not affected by the increase in average distance between integral proteins (60). The following two models can explain the above phenomenon. Model 1 is that cytochrome bc_1 complex, cytochrome *c*, and cytochrome oxidase are independent diffusible components and cytochrome *c* shuttles very rapidly between the two components, so that diffusion of cytochrome oxidase and cytochrome bc_1 complex in the membrane is not the rate-limiting step in electron transfer (see Fig. 8). Model 2 is that the electron transfer segment from cytochrome *b* to cyto-

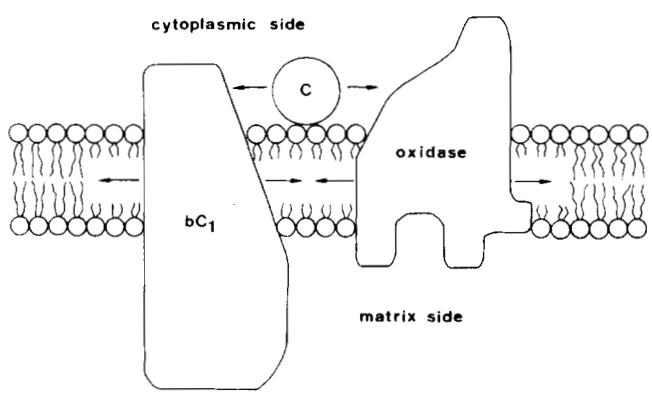

FIG. 8. **Schematic model illustrating electron transfer between cytochrome bc_1 complex and cytochrome oxidase.** Cytochrome *c* (*c*) shuttles rapidly between independently diffusing cytochrome bc_1 complex (bc_1) and cytochrome oxidase (*oxidase*) along the membrane surface of the cytoplasmic side. This model is based on the present results of bc_1-oxidase interactions in co-reconstituted lipid vesicles.

chrome oxidase diffuses as one structural entity. Since we failed to observe any specific interaction between cytochrome bc_1 complex and cytochrome oxidase, the former model appears more likely. Rieder and Bosshard (62, 63) have shown that the binding sites on cytochrome *c* for cytochrome oxidase, cytochrome bc_1 complex, and purified cytochrome c_1 are indistinguishable, also implying that cytochrome *c* may not form a supermolecular complex at the same time with both cytochrome oxidase and the c_1 subunit of cytochrome bc_1 complex. As discussed already, the probable high rate of lateral diffusion for peripheral cytochrome *c* on membranes could support Model 1. The stoichiometry of heme components in the mitochondrial membrane was reported as heme (2b + c_1):heme c:heme aa_3 = 3:7:7 (12), 1:2:2 (64), and 1:6:6 (65). Although no agreement is achieved in the above stoichiometry, the amount of heme (2b + c_1) is less than one-half of that of heme c and heme aa_3, suggesting that Model 2 is less realistic. Thus, it is most likely that electrons are transferred by lateral collisions of cytochrome *c* with cytochrome bc_1 complex or cytochrome oxidase.

CONCLUSION

The present investigations of rotation of cytochrome oxidase in PE-PC-CL vesicles reveal the following properties: 1) rotation of the whole cytochrome oxidase molecule only occurs about the normal to the plane of the membrane. 2) Nearly all standard cytochrome oxidase rotates in high L/P $\simeq$ 27 vesicles. About 20% of standard cytochrome oxidase is immobile in low L/P $\simeq$ 5 vesicles in both the presence and absence of cytochrome bc_1 complex. Thus, an increase in the enzyme concentration in the membrane induces an immobilization of cytochrome oxidase which is presumably due to nonspecific protein aggregation. A high concentration of enzymes in the inner mitochondrial membrane is a possible cause of the rotational immobilization of about one-half of cytochrome oxidase molecules. 3) 30% of column-purified cytochrome oxidase is immobile in L/P $\simeq$ 27 vesicles. 4) No specific supermolecular complex is formed between cytochrome oxidase and cytochrome bc_1 complex. This suggests that local lateral diffusion and collisions may play an essential role for electron transfer from cytochrome bc_1 complex to cytochrome oxidase through cytochrome *c* in the inner membrane of mitochondria.

Acknowledgments—We are greatly indebted to M. Müller for freeze-fracture and negative stain electron micrograph measurements and to C. Zugliani for technical assistance.

REFERENCES

1. Boyer, P. D., Chance, B., Ernster, L., Mitchell, P., Racker, E., and Slater, E.C. (1977) *Annu. Rev. Biochem.* **46,** 955–1026
2. Chance, B., Lee, C. P., Mela, L., and Devault, D. (1968) in *Structure and Functions of Cytochromes* (Okunuki, K., Kamen, M. D., and Sekuzu, I., eds) p. 475, University of Tokyo Press, Tokyo
3. Ludwig, B., Downer, N. W., and Capaldi, R. A. (1979) *Biochemistry* **18,** 1401–1407
4. Orii, Y. (1979) in *Cytochrome Oxidase* (King, T. E., Orii, Y., Chance, B., and Okunuki, K., eds) pp. 331–340, Elsevier/North-Holland, Amsterdam
5. Wikström, M. K. F., and Saari, H. T. (1977) *Biochim. Biophys. Acta* **462,** 347–361
6. Wikström, M., and Krab, K. (1978) *FEBS Lett.* **91,** 8–14
7. Sigel, E., and Carafoli, E. (1978) *Eur. J. Biochem.* **89,** 119–123
8. Sigel, E., and Carafoli, E. (1979) *J. Biol. Chem.* **254,** 10572–10574
9. Erecińska, M., and Wilson, D. F. (1978) *Arch. Biochem. Biophys.* **188,** 1–14
10. Rieske, J. S. (1976) *Biochim. Biophys. Acta* **456,** 195–247
11. Mitchell, P. (1966) *Biol. Rev.* **41,** 445–502
12. Hatefi, Y., Galante, Y. M., Stiggall, D. L., and Ragan, C. I. (1979) *Methods Enzymol.* **56,** 577–602
13. Leung, K. H., and Hinkle, P. C. (1975) *J. Biol. Chem.* **250,** 8467–8471
14. Mitchell, P. (1975) *FEBS Lett.* **56,** 1–6
15. Höchli, M., and Hackenbrock, C. R. (1976) *Proc. Natl. Acad. Sci. U. S. A.* **73,** 1636–1640
16. Höchli, M., and Hackenbrock, C. R. (1979) *Proc. Natl. Acad. Sci. U. S. A.* **76,** 1236–1240
17. Kawato, S., Sigel, E., Carafoli, E., and Cherry, R. J. (1980) *J. Biol. Chem.* **255,** 5508–5510
18. Ariano, H. A., and Azzi, A. (1980) *Biochem. Biophys. Res. Commun.* **93,** 478–485
19. Swanson, M. S., Quintanilha, A. T., and Thomas, D. D. (1980) *J. Biol. Chem.* **255,** 7494–7502
20. Nigg, E. A., and Cherry, R. J. (1980) *Proc. Natl. Acad. Sci. U. S. A.* **77,** 4702–4706
21. Cherry, R. J., and Godfrey, R. E. (1981) *Biophys. J.*, in press
22. Junge, W., and DeVault, D. (1975) *Biochim. Biophys. Acta* **408,** 200–214
23. Carroll, R. C., and Racker, E. (1977) *J. Biol. Chem.* **252,** 6981–6990
24. Eytan, G. D., and Broza, R. (1978) *J. Biol. Chem.* **253,** 3196–3202
25. Yoshida, S., Orii, Y., Kawato, S., and Ikegami, A. (1979) *J. Biochem. (Tokyo)* **86,** 1443–1450
26. Denes, A. S., and Stanacev, N. Z. (1979) *Can. J. Biochem.* **57,** 238–249
27. Kawato, S., Ikegami, A., Yoshida, S., and Orii, Y. (1980) *Biochemistry* **19,** 1598–1603
28. Kawato, S., Yoshida, S., Ikegami, A., Orii, Y., and Kinosita, K., Jr. (1981) *Biochim. Biophys. Acta* **634,** 85–92
29. Krebs, J. J. R., Hauser, H., and Carafoli, E. (1979) *J. Biol. Chem.* **254,** 5308–5316
30. Yonetani, T. (1967) *Methods Enzymol.* **10,** 742–745
31. Rieska, J. S. (1967) *Methods Enzymol.* **10,** 239–245
32. Brunner, J., Hauser, H., and Semenza, G. (1978) *J. Biol. Chem.* **253,** 7538–7546
33. Miller, C., and Racker, E. (1976) *J. Membr. Biol.* **26,** 319–333
34. Chen, P. S., Toribara, T. V., and Huber, W. (1956) *Anal. Chem.* **28,** 1756–1758
35. Sigel, E., and Carafoli, E. (1980) *Eur. J. Biochem.* **111,** 299–306
36. Guerrieri, F., and Nelson, B. D. (1975) *FEBS Lett.* **54,** 339–342
37. Hinkle, P. C., Kim, J. J., and Racker, E. (1972) *J. Biol. Chem.* **247,** 1338–1339
38. Moor, H., Kistler, J., and Müller, M. (1976) *Experientia* **32,** 805
39. Cherry, R. J. (1978) *Methods Enzymol.* **54,** 47–61
40. Henderson, R., Capaldi, R. A., and Leigh, J. S. (1977) *J. Mol. Biol.* **112,** 631–648
41. Kawato, S., and Kinosita, K., Jr. (1981) *Biophys. J.*, in press
42. Kunze, U., and Junge, W. (1977) *FEBS Lett.* **80,** 429–434
43. Junge, W., and Eckhof, A. (1974) *Biochim. Biophys. Acta* **357,** 103–117
44. Racker, E. (1972) *J. Membr. Biol.* **10,** 221–235
45. Blasie, J. K., Erecińska, M., Samuels, S., and Leigh, J. S. (1978) *Biochim. Biophys. Acta* **501,** 33–52
46. Erecińska, M., Wilson, D. F., and Blasie, J. K. (1978) *Biochim. Biophys. Acta* **501,** 53–62
47. Saffman, P. G., and Delbrück, M. (1975) *Proc. Natl. Acad. Sci. U. S. A.* **72,** 3111–3113
48. Wingfield, P., Arad, T., Leonard, K. R. and Weiss, H. (1979) *Nature* **280,** 696–697
49. Leonard, K. R., Arad, T., Wingfield, P., and Weiss, H. (1980) in *First European Bioenergetics Conference*, pp. 83–84, Patron Editore, Bologna
50. Fuller, S. D., Capaldi, R. A., and Henderson, R. (1979) *J. Mol. Biol.* **134,** 305–327
51. Orii, Y., and Yoshikawa, S. (1973) in *Oxidase and Related Redox Systems* (King, T. E., Mason, H. S., and Morrison, M., eds) pp. 649–675, University Park Press, Baltimore
52. Axelrod, D., Koppel, D. E., Schlessinger, J., Elson, E., and Webb, W. W. (1976) *Biophys. J.* **16,** 1055–1069
53. Axelrod, D., Wight, A., Webb, W. W., and Horwitz, A. (1978) *Biochemistry* **17,** 3604–3609
54. Smith, L. M., Smith, B. A., and McConnell, H. M. (1979) *Biochemistry* **18,** 2256–2259
55. Golbeau, A., Nachbaur, J., and Vignais, P. M. (1971) *Biochim. Biophys. Acta* **249,** 462–492
56. Harmon, H. J., Hall, J. D., and Crane, F. L. (1974) *Biochim. Biophys. Acta* **344,** 119–155
57. Vanderkooi, G. (1974) *Biochim. Biophys. Acta* **344,** 307–345

58. Cherry, R. J. (1979) *Biochim. Biophys. Acta* **559,** 289-327
59. Vaz, W. L. C., Jacobson, K., Wu, E-S., and Derzko, Z. (1979) *Proc. Natl. Acad. Sci. U. S. A.* **76,** 5645-5649
60. Schneider, H., Lemasters, J. J., Höchli, M., and Hackenbrock, C. R. (1980) *J. Biol. Chem.* **255,** 3748-3756
61. Schneider, H., Lemasters, J. J., Höchli, M., and Hackenbrock, C. R. (1980) *Proc. Natl. Acad. Sci. U. S. A.* **77,** 442-446
62. Rieder, R., and Bosshard, H. R. (1978) *J. Biol. Chem.* **253,** 6045-6053
63. Rieder, R., and Bosshard, H. R. (1980) *J. Biol. Chem.* **255,** 4732-4739
64. Slater, E. C. (1972) in *Mitochondria and Biomembranes* (Van Den Bergh, S. G., Borst, P., Van Deenen, L. L. M., Riemersma, J. C., Slater, E. C., and Tager, J. M., eds) pp. 133-146, Elsevier/North-Holland, Amsterdam
65. Kagawa, Y. (1978) *Biomembranes*, p. 222, Iwanami, Tokyo

SUPPLEMENTARY MATERIAL TO

ROTATION OF CYTOCHROME OXIDASE IN PHOSPHOLIPID VESICLES: INVESTIGATIONS OF INTERACTIONS BETWEEN CYTOCHROME OXIDASES AND BETWEEN CYTOCHROME OXIDASE AND CYTOCHROME bc_1 COMPLEX

Suguru Kawato, Erwin Sigel, Ernesto Carafoli and Richard J. Cherry

Theoretical Treatment of Rotation of Cytochrome Oxidase in Membranes

Cytochrome oxidase maintains a fixed orientation with respect to the sideness of the membrane (3,40), implying that rotation occurs about the normal to the plane of the membrane. As has been shown by Kunze and Junge (42), it is necessary to consider the ellipticity of the heme a_3 chromophore. A theoretical treatment of this case for heme proteins shows that the expected form of r(t) for a weak photoselection flash is given by (41):

$$r(t)/r(0) = A_1\exp(-t/\phi_{//}) + A_2\exp(-4t/\phi_{//}) + A_3 \qquad (1)$$

$$A_1 = \frac{1}{Q}\left[\sin^2\theta_{H_1}\cos^2\theta_{H_1} - (c_e^2+c_m^2)\cos^2\theta_{H_1}\cos^2\theta_{H_2} + c_e^2c_m^2\sin^2\theta_{H_2}\cos^2\theta_{H_2}\right] \qquad (2)$$

$$A_2 = \frac{1}{4Q}\left[\sin^4\theta_{H_1} - (c_e^2+c_m^2)(2\cos^2\theta_{H_1}\cos^2\theta_{H_2} - \sin^2\theta_{H_1}\sin^2\theta_{H_2}) + c_e^2c_m^2\sin^4\theta_{H_2}\right] \qquad (3)$$

$$A_3 = \frac{1}{4Q}\left[(3\cos^2\theta_{H_1}-1)^2 + (c_e^2+c_m^2)(3\cos^2\theta_{H_1}-1)(3\cos^2\theta_{H_2}-1) + c_e^2c_m^2(3\cos^2\theta_{H_2}-1)^2\right] \qquad (4)$$

$$r(0) = 0.4Q/(c_e^2+1)(c_m^2+1) \qquad (5)$$

$$Q = c_e^2c_m^2 - (c_e^2+c_m^2)/2 + 1 \qquad (6)$$

where $\phi_{//}$ is the rotational relaxation time about the membrane normal ($\phi_{//} = 1/D_{//}$, $D_{//}$ is the rotational diffusion coefficient), θ_{H_i} (i=1,2) the angle between **n** and the absorption moment $\mathbf{H}_1$ or $c\mathbf{H}_2$ which lie in the heme plane, $c_e\mathbf{H}_2$ and $c_m\mathbf{H}_2$ represent $c\mathbf{H}_2$ at the excitation wavelength and measurement wavelength, respectively. Here we assume that the heme plane has two absorption moments $\mathbf{H}_1$, $c\mathbf{H}_2$ which lie in the heme plane with right angles to one another ($|\mathbf{H}_1|^2=|\mathbf{H}_2|^2=1$).

When the heme chromophore has a 4-fold symmetry at both the excitation and measurement wavelengths (i.e. $c_e=c_m=1$), r(t) simplifies to:

$$r(t)/r(0) \equiv r(t)/0.1 = \tfrac{3}{4}\sin^2\theta_N\cos^2\theta_N\exp(-t/\phi_{//}) + \tfrac{3}{4}\sin^4\theta_N\exp(-4t/\phi_{//}) + \tfrac{1}{4}(3\cos^2\theta_N-1)^2 \qquad (7)$$

where we assume a single rotating species, θ_N is the angle between **n** and the normal to the heme plane **N**. One should note that for 4-fold symmetry, although r(0) depends on the intensity of excitation flash, r(t)/r(0) is independent of the flash intensity (41). Thus the theoretical analysis of data is more straightforward and can be quantitative in the case of circular degeneracy. It is therefore important to find out the wavelength at which the heme a_3 chromophore has an effective 4-fold symmetry.

Since the heme a_3·CO chromophore has been shown to be circularly degenerate at about 591 nm (42), at the present excitation wavelength of 530 ± 1 nm 4-fold symmetry should be approximately valid (i.e. $c_e \simeq 1$). Equation 7 predicts that, when the heme a_3 chromophore is circularly degenerate at the measurement wavelength (i.e. $c_m=1$), r(0) should be 0.1. We scanned the measurement wavelength from 446 to 448 nm and determined the correct r(0) value with a very weak excitation flash in order to prevent a decrease in r(0) induced by the intense flash excitation (41). Figure 4A shows that at about 447 nm the heme a_3 chromophore has a 4-fold symmetry (i.e. $c_m=1$). A possible decrease in r(0) due to the presence of 60% D-sucrose, which has a specific rotation of $[\alpha]_D^{20}$=66-67°, in our sample was negligible, since we observed no increase in r(0) in the mixture of 30% D-sucrose and 30% L-glucose solution compared with r(0) in 60% D-sucrose solution within experimental error ($[\alpha]_D^{20}$=-64° for L-glucose).

The wavelength dependence of the whole r(t) curve was also examined by analyzing data with the following equation:

$$r(t) = r_1\exp(-t/\phi_1) + r_2\exp(-4t/\phi_1) + r_3 \qquad (8)$$

A typical example of r(t)'s at different wavelengths is shown in Figure 4B. Although individual r_i's are dependent on the measurement wavelength, $r_i/r(0)$ (i=1,2,3) and ϕ_1 remain unchanged over 446-448 nm within experimental error. We often used 446 nm for actual r(t) measurements, since between 446 and 448 nm signal to noise is best at 446 nm, where the total absorbance change A(t) is largest.

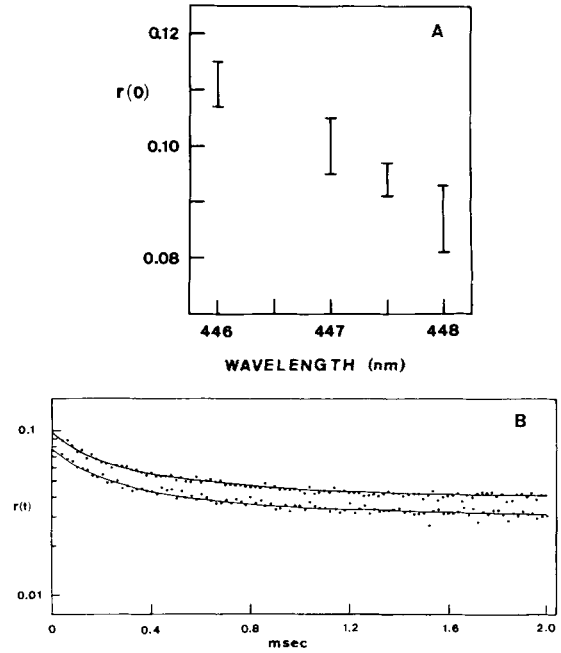

Figure 4 Wavelength dependence of the absorption anisotropy of the cytochrome oxidase·CO complex. Samples (4 μM in heme a) were photolysed by a vertically polarized laser flash at 590 nm, and r(t) was recorded at 446-448 nm as described under "Experimental Procedures". All measurements were performed with Ca^{2+}-fused pellet vesicles in 60% sucrose solution at 20 °C (58 cP).

(4A) The initial anisotropy $r(0) = r_1+r_2+r_3$ was calculated by fitting the data to Equation 8. Vertical bars in the figure represent the spread of measured values of r(0). The fraction of excited heme chromophores was kept less than 7% in these r(0) measurements, so that the deviation of r(0) from the ideal case (zero excitation flash intensity) should be less than 5% (41).

(4B) Upper curve: r(t) measured at 446 nm. Lower curve: r(t) measured at 448 nm. Solid lines were obtained by fitting the data to Equation 8.